5482–5490 *Nucleic Acids Research, 2006, Vol. 34, No. 19* *Published online 4 October 2006*
doi:10.1093/nar/gkl701

Controlling bacteriophage phi29 DNA-packaging motor by addition or discharge of a peptide at N-terminus of connector protein that interacts with pRNA

Jianhe Sun[1,2], Ying Cai[1], Wulf-Dieter Moll[1] and Peixuan Guo[1,*]

[1]Department of Pathobiology, Purdue Cancer Center and Weldon School of Biomedical Engineering, Purdue University, West Lafayette, IN 47907, USA and [2]School of Agriculture and Biology, Shanghai Jiaotong University, Shanghai, 201101, People's Republic of China

Received July 12, 2006; Revised September 1, 2006; Accepted September 6, 2006

ABSTRACT

Bacteriophage phi29 utilizes a motor to translocate genomic DNA into a preformed procapsid. The motor contains six pRNAs, an enzyme and one 12-subunit connector with a central channel for DNA transportation. A 20-residue peptide containing a His-tag was fused to the N-terminus of the connector protein gp10. This fusion neither interfered with procapsid assembly nor affected the morphology of the prolate-shaped procapsid. However, the pRNA binding and virion assembly activity were greatly reduced. Such decreased functions can be switched back on by the removal of the tag via protease cleavage, supporting the previous finding that the N-terminus of gp10 is essential for the pRNA binding. The DNA-packaging efficiency with dimeric pRNA was more seriously affected by the extension than with monomeric pRNA. It is speculated that the fusion of the tag generated physical hindrance to pRNA binding, with greater influence for the dimers than the monomers due to their size. These results reveal a potential to turn off and turn on the motor by attaching or removing, respectively, a component to outer part of the motor, and offers an approach for the inhibition of viral replication by using a drug or a small peptide targeted to motor components.

INTRODUCTION

The viral DNA-packaging motor of dsDNA bacteriophage (e.g. phi29, lambda, T4 and T7) can translocate and compress genomic DNA with tremendous velocity into a preformed protein shell, called the procapsid, fueled by hydrolysis of ATP during assembly (1–6). The procapsid of *Bacillus subtilis* bacteriophage phi29 consists of the major capsid protein gp8 (235 copies), connector protein gp10 (12 copies), head fiber protein gp8.5 (55 copies) and the scaffolding protein gp7 (180 copies) (7–9). Investigation of the bacterial virus phi29 DNA-packaging motor revealed a molecule known as pRNA (packaging RNA) that plays an essential role in packaging DNA into procapsid (10). The pRNA contains two functional domains (Figure 1A) (11,12). One domain, composed of the central region of the pRNA, binds to the procapsid. The other domain, which functions as a DNA translocation domain, is located at the 5′/3′ paired ends. Six copies of pRNA have been hypothesized to form a hexameric ring via monomer to dimer and then hexamer (13–15) to drive the DNA-packaging motor.

One of the essential components of the phi29 DNA-packaging motor is the connector complex, which shows a dodecameric cylindrical structure with a 3.6 nm central channel through which viral genomic DNA is packaged into or exits the procapsid during the viral life cycle. The detailed structure of the phi29 portal connector protein gp10 has been solved at the atomic resolution (16,17). The phi29 connector ring consists of alpha-helical subunits, and three long helices of each subunit form an inner channel. The wider end of the connector is kept inside the procapsid, while the narrow end partially protrudes from the procapsid. Based upon the structure, it is evident that the N-terminus protrudes from the narrow end of the connector and the C-terminus extends from the wider end of the connector (Figure 1B) (16–20); therefore, the C-terminus is hidden within the procapsid and the N-terminus is exposed to the solvent.

Recent DNA-packaging models proposed that the 5-fold procapsid vertex and 12-fold connector (or the hexameric

*To whom correspondence should be addressed at Purdue Cancer Center, B-36 Hansen Life Science Research Building, Purdue University, West Lafayette, IN 47907, USA. Tel: +1 765 494 7561; Fax: +1 765 496 1795; Email: guop@purdue.edu
Present address:
Wulf-Dieter Moll, Department for Agrobiotechnology, IFA-Tulln, University of Natural Resources and Applied Life Sciences, Vienna, Austria

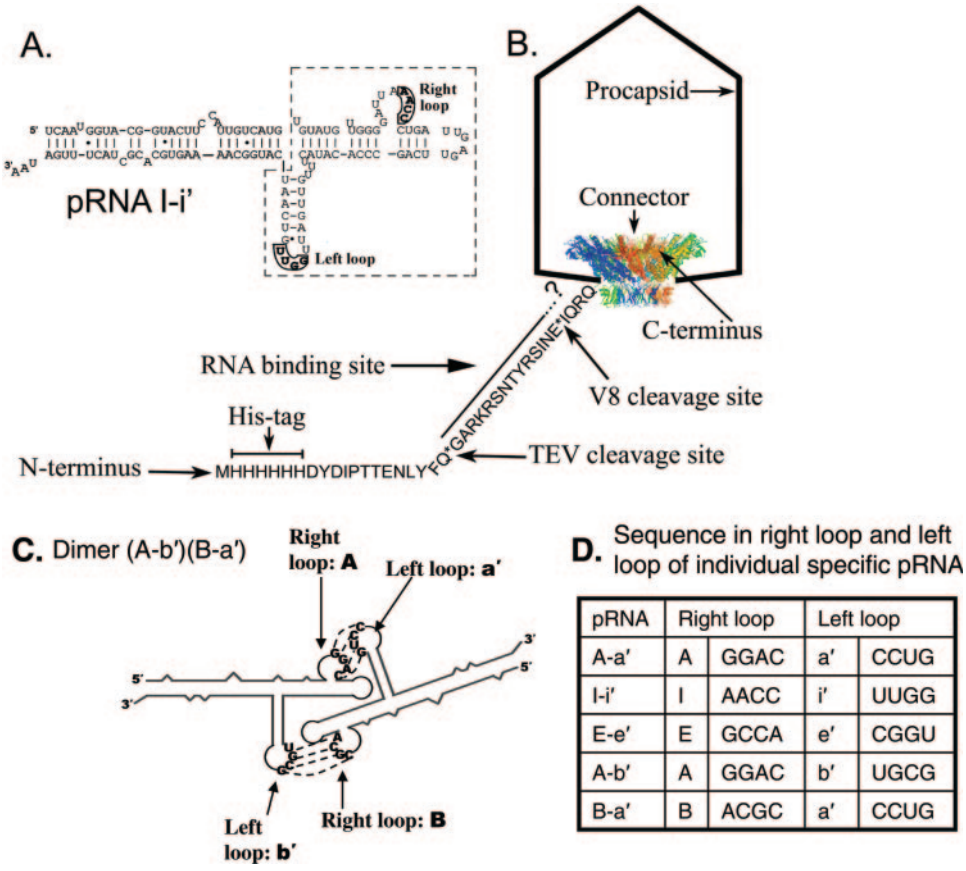

pRNA	Right loop		Left loop	
A-a′	A	GGAC	a′	CCUG
I-i′	I	AACC	i′	UUGG
E-e′	E	GCCA	e′	CGGU
A-b′	A	GGAC	b′	UGCG
B-a′	B	ACGC	a′	CCUG

Figure 1. Schematic presentation of protease TEV cleavage site, V8 cleavage site at the N-terminus of connector in His-procapsid, primary sequences and secondary structure of wild-type phenotype pRNA I-i′. (**A**) Primary sequences and predicted secondary structure of wild-type phenotype pRNA I-i′. Right and left loops involved in hand-in-hand interaction are boxed and in boldface. Two functional domains are outlined. (**B**) TEV cleavage site, V8 cleavage site and amino acid sequence at the N-terminal of His-gp10 as shown in a His-procapsid model. (**C**) Illustration for the formation of a pRNA dimer (A-b′) (B-a′) via interlocking right and left loop. (**D**) Sequence in the right loop and left loop of individual specific pRNA.

pRNA ring) could constitute a mechanical motor in which the relative motion of the two rings could produce a force to drive the phi29 rotation motor to pack DNA (17,19–21). Although the published DNA-packaging models all agree that pRNA bound to one component to execute a consecutive rotation (17,20,21), there were discrepancies regarding the foothold for the pRNA. The recently published data (22) suggest that the foothold for pRNA binding is the connector, specifically, the N-terminus. Six copies of pRNA are bound to the connector and work sequentially, so that the pRNA–connector complex is part of the rotor (21).

In this study, we demonstrate that an additional 20 amino acids fused to the N-terminus of gp10 did not morphologically affect procapsid assembly but blocked the binding of pRNA to the His-procapsid. However, such diminished function can be switched 'on' by the removal of the 20 amino acids via proteolytic cleavage with Tobacco Etch Virus (TEV) protease. These results reveal a potential to turn on and off the motor by attaching a component to the N-terminus of the connector, and offers an approach for the inhibition of viral replication using a drug or a small peptide targeted to motor components for specific blockage of DNA-packaging.

MATERIALS AND METHODS

Construction of plasmid pHis-gp7-8-8.5-10 for the production of recombinant His-procapsid

Plasmid pHis-gp7-8-8.5-10 was constructed from two plasmids, pET-His-gp10 (23) and pARgp7-8-8.5 (24). Plasmid pARgp7-8-8.5 was digested with *Bam*H I and *Bgl* II, generating a DNA fragment containing gp7-8-8.5 with two cohesive ends both compatible with *Bgl* II. This fragment was inserted into the *Bgl* II site of pET-His-gp10, resulting in a His-procapsid expression vector pHis-gp7-8-8.5-10.

Expression and purification of His-procapsid

To express and purify His-procapsid, an *Escherichia coli* strain harboring the plasmid pHis-gp7-8-8.5-10 coding for His-gp7-8-8.5-10 was inoculated into 5 ml Luria–Bertani (LB) medium containing 100 μg/ml ampicillin and grown overnight at 37°C with vigorous shaking (200 r.p.m.). Overnight seed culture (5 ml) was inoculated into 500 ml LB medium containing 100 μg/ml ampicillin and grown at 37°C with vigorous shaking, followed by 0.5 mM IPTG induction for 3 h when OD_{600} reached 0.5–0.6. The cells

were harvested by centrifugation with a JS-7.5 rotor (Beckman) at 6500 r.p.m., 4°C for 15 min, and resuspended in 25 ml lysate in buffer A (50 mM Tris–HCl, pH 8.0, 50 mM NaCl, 1 mM EDTA, pH 8.0, 2 mM DTT and 1 mM PMSF). Cell lysate was obtained by French Press at 10K psi twice, followed by centrifugation at 10 000 r.p.m. (JA-20, Beckman), 4°C for 30 min. The supernatant was loaded onto the step gradient of 20–40% Optiprep and centrifuged at 40 000 r.p.m., 4°C for 12 h with a Ti45 rotor (Beckman). A thick band of concentrated prohead cell lysate was collected and further resuspended into TBE buffer (89 mM Tris–borate and 2 mM EDTA, pH 8.0) with 4-fold dilution, and then collected by centrifugation at 35 000 r.p.m., 4°C for 2 h with a SW55 rotor (Beckman). The pellets were resuspended in 300 µl TMS buffer (50 mM Tris–HCl, pH 7.8, 100 mM NaCl and 10 mM $MgCl_2$), and sonicated for 40 s. The His-procapsid was isolated by centrifugation in 10–30% (w/v) linear sucrose gradients prepared in TMS buffer with a SW28 rotor (Beckman), at 25 000 r.p.m., 4°C for 4.5 h. After the His-procapsid band was collected and the particles were spun down at 35 000 r.p.m., 4°C for 2 h with a SW55 rotor (Beckman), and resuspended in 200 µl TMS buffer and sonicated for 40 s. Wild-type procapsid was also expressed and purified with exactly the same procedure. The purified His-procapsid and procapsid were confirmed and quantified with 10% SDS–PAGE.

Proteolytic treatment of His-procapsid

The purified His-procapsid was treated by TEV with an enzyme/substrate molar ratio of ~1:20 for 16 h at 4°C. Procapsid was treated in the same manner as the His-procapsid. The proteolytic efficiency was determined with 10% SDS–PAGE.

Electron microscopy of His-procapsid

Carbon-coated TEM grids were made hydrophilic by glow discharge and floated for 1 min on drops of His-procapsid, which were purified from a 10–30% sucrose gradient centrifugation and resuspended in TMS. The grids were negative-stained with 2% uranyl acetate. Electron micrographs were taken on a Philips CM-100 transmission electron microscope. Same procedures were used for TEV cleaved His-procapsid and wild-type procapsid.

Synthesis of pRNA

The pRNA I-i′, A-a′, *Sph* I I-i′, *Sph* I A-a′, *Sph* I E-e′, *Sph* I A-b′ and *Sph* I B-a′ were synthesized by *in vitro* transcription with T7 RNA polymerase from a PCR-generated template, as described previously (11,25,26). RNA with a prefix *Sph* I is the RNA with a 26 base extension at the 3′ end. Radiolabeled pRNA such as [^{3}H]pRNA I-i′ and [^{3}H]pRNA A-a′ were prepared by including [^{3}H]UTP (Amersham) in the transcription reaction.

Binding assays for pRNAs to His-procapsid and procapsid

Binding assays were performed with sucrose gradient sedimentation. A constant amount (8 µg) of purified His-procapsid, TEV cleaved His-procapsid or procapsid, was mixed with 100 ng of different types of ^{3}H-labeled pRNA ([^{3}H]*Sph* I I-i′ and [^{3}H]pRNA A-a′) in TMS buffer, respectively, and then dialyzed on a 0.25 µm VS filter membrane (Millipore Corp.) against TBE buffer for 15 min at the ambient temperature. The mixtures containing procapsid (or His-procapsid) and pRNA were further dialyzed against TMS buffer for another 30 min at the ambient temperature and then loaded onto a 5–20% sucrose gradient in TMS. After 35 min of centrifugation in a SW55 rotor (Beckman) at 35 000 r.p.m. at the ambient temperature, fractions were collected 10 drops each from the bottom of the tube and subjected to liquid scintillation counting.

In vitro phi29 DNA-packaging and viral assembly to determine the activity of His-procapsid

The *in vitro* assembly of phi29 virion with pRNA, ATPase gp16, phi29 DNA-gp3, procapsid, and with supply of final 1 mM ATP in TMS buffer have been described previously (27).

Determination of the requirement of pRNA for DNA-packaging with His-procapsid

To confirm the presence of the His-procapsid–pRNA complex, it is necessary to remove free pRNA from the presumed His-procapsid–pRNA complex. His-procapsid (15 µg) was mixed with 500 ng pRNA of *Sph* I I-i′ in TMS buffer, and then dialyzed on a 0.25 µm pore size type VS filter membrane (Millipore Corp.) against TBE buffer for 15 min, followed by dialysis against TMS buffer for another 30 min at ambient temperature. The mixture was loaded onto a 5–20% sucrose gradient in TMS. After 35 min of centrifugation in an SW55 rotor (Beckman) at 35 000 r.p.m. at 9°C, fractions corresponding to the presumed His-procapsids–pRNA complex were collected and then loaded onto 4.5 ml 10% sucrose in TMS buffer, the presumed His-procapsid–pRNA complex were sedimented by ultracentrifugation in an SW55 rotor (Beckman) at 35 000 r.p.m. at 20°C for 2 h. The buffer containing free pRNA was removed by aspiration carefully, and the sedimented complex was resuspended in 50 µl TMS buffer. The presumed His-procapsid–pRNAcomplex were then treated with RNase A, or untreated, and used to detect the virion assembly activity.

RESULTS

Plasmid construction, structural gene expression and purification of recombinant His-procapsid containing His-tagged connector protein gp10

Procapsid proteins gp7, gp8, gp8.5 and His-gp10 were co-expressed in *E.coli* cells, harboring the plasmid pHis-gp7-8-8.5-10. These proteins self-assembled into His-procapsid. After purification, the His-tagged procapsid was analyzed with SDS–PAGE, revealing that all the procapsid structural components gp7, gp8, gp8.5 and gp10 of the His-procapsid were present with a similar ratio as compared to wild-type phi29 procapsid. The molecular weight of gp7, gp8 and gp8.5 were identical to the corresponding proteins in wild-type procapsid, while His-gp10 showed higher molecular weight than wild-type gp10 due to the 20 additional amino acids (Figure 2). His-procapsid, His-procapsid cleaved by

TEV and wild-type procapsid were examined by negative stain electron microscopy. Results showed that there were no significant changes in the structure among them; all showed the typical prolate-shape of phi29 procapsid (Figure 3), suggesting that the His-procapsid possesses the same morphology as procapsid assembled from untagged gp10 (Figure 3A).

Proteolytic treatment of His-procapsid generated wild-type procapsid

In the procapsid, the C-terminus of gp10 is located at the wider end of the connector that is buried within the procapsid, while the N-terminus is located at the narrow end of the connector that is exposed to the solvent. Protease TEV is expected to cleave the His-tag that is fused with the TEV recognition site proximal to the N-terminus of gp10 (Figure 1B). Treatment of His-procapsid with TEV resulted in the removal of His-tag, producing a gp10 with molecular weight similar to the gp10 from wild-type procapsid (Figure 2). SDS-PAGE analysis of the protein profile of His-procapsid after TEV digestion confirmed the cleavage of His-gp10 into wild-type gp10, while no changes were observed for the major capsid protein gp8, the fiber protein gp8.5 and the scaffolding protein gp7 of the procapsid (Figure 2). The results indicate that TEV cleaved His-procapsid produced a procapsid with a normal connector protein gp10 without affecting other capsid proteins.

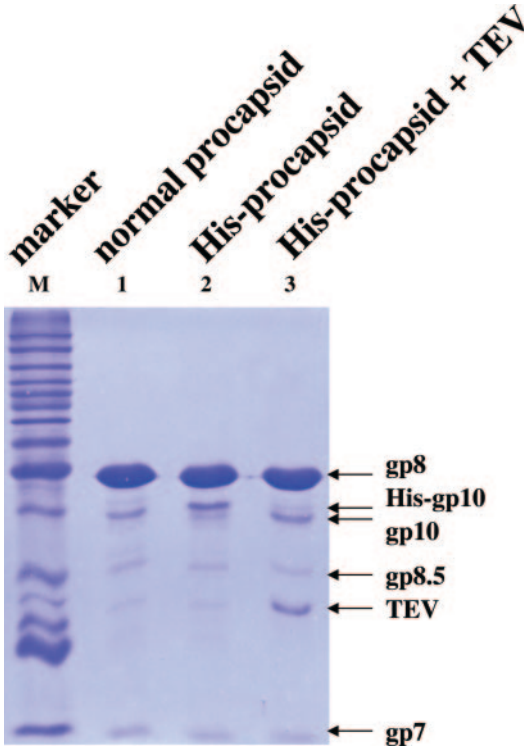

Figure 2. SDS–PAGE (10%) profile of the His-procapsid before and after TEV cleavage.

The activities for pRNA binding, DNA-packaging and virion assembly of His-procapsid were decreased for His-procapsid compared to wild-type procapsid

The inhibition by the His-procapsid in pRNA binding was clearly shown by sucrose gradient sedimentation. The purified His-procapsid was incubated with [^{3}H]pRNA and then subjected to 5–20% sucrose gradient sedimentation. Results showed that the binding of pRNA to His-procapsid was almost undetectable. No radioactive peak for His-procapsid–pRNA complex could be found, while a peak representing the normal procapsid–pRNA complex appeared and was centered near fraction 22 when procapsid was mixed with [^{3}H]pRNA (Figure 4).

An *in vitro* DNA-packaging system was used to test whether the His-procapsid is functional in DNA translocation. The results showed that the efficiency of DNA-packaging into His-procapsid decreased only 2- to 5-fold when using pRNA A-a′, *Sph* I A-a′, *Sph* I E-e′ or *Sph* I A-b′+ *Sph* I B-a′ in the packaging assay (Figures 5 and 6B). Viral assembly activity of His-procapsid was assayed by plaque formation analyzed with the highly sensitive phi29 assembly system. It was found that phi29 assembly activity was reduced more than 10-fold in the presence of an additional 20 amino acids at the N-terminus of the connector (Figure 7).

In conclusion, the insertion of a His-tag to the N-terminal of gp10 significantly interfered with the binding of pRNA to procapsid, resulting in binding of pRNA to procapsid almost undetectable (>99% reduction) by sucrose gradient sedimentation (Figure 4). However, <5% reduction of DNA-packaging activity was observed when pRNA I-i′ was used (Figure 6B), and ~10-fold reduction in viral assembly was observed (Figure 8).

The activity for pRNA binding, DNA-packaging and viral assembly activity of the His-procapsid were restored after the removal of the 20 amino acids by proteolytic cleavage

TEV cleavage of His-procapsid restored its activity for pRNA binding (Figure 4). The diminished DNA-packaging activity

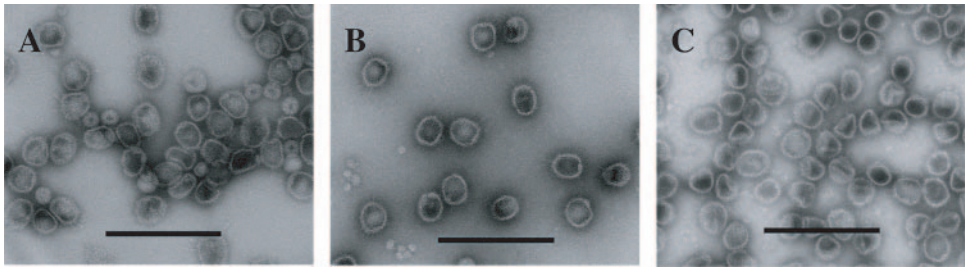

Figure 3. Electron micrographs of negative-stained procapsids. (**A**) His-procapsid. (**B**) His-procapsid cleaved with TEV. (**C**) Procapsid. Bar = 200 nm.

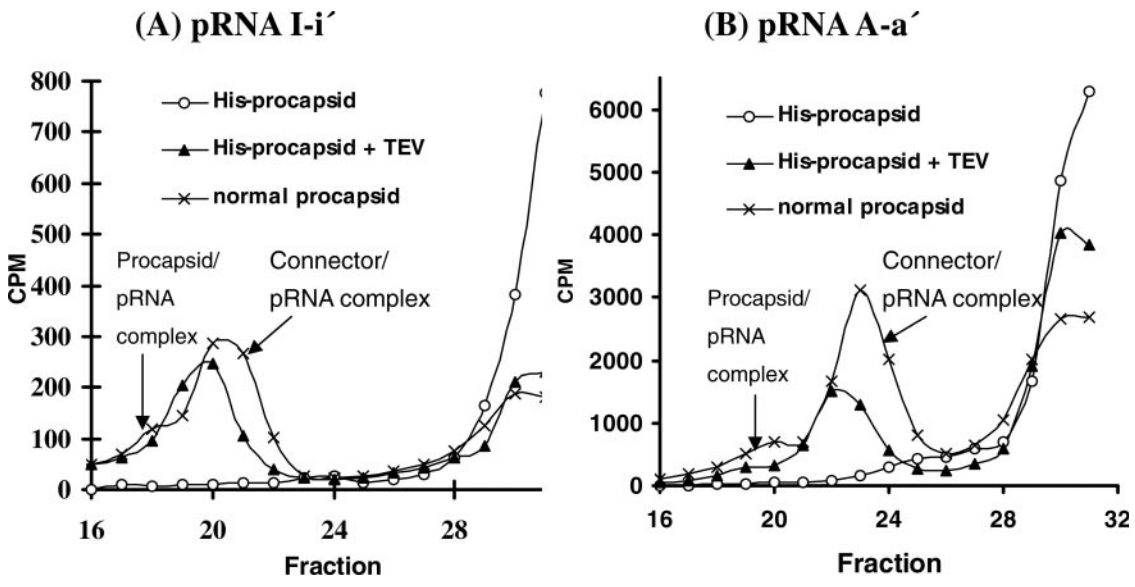

Figure 4. Sucrose gradient (5–20%) sedimentation to detect the binding of His-procapsid with ^{3}H-labeled pRNA (**A**) I-i′; (**B**) A-a′.

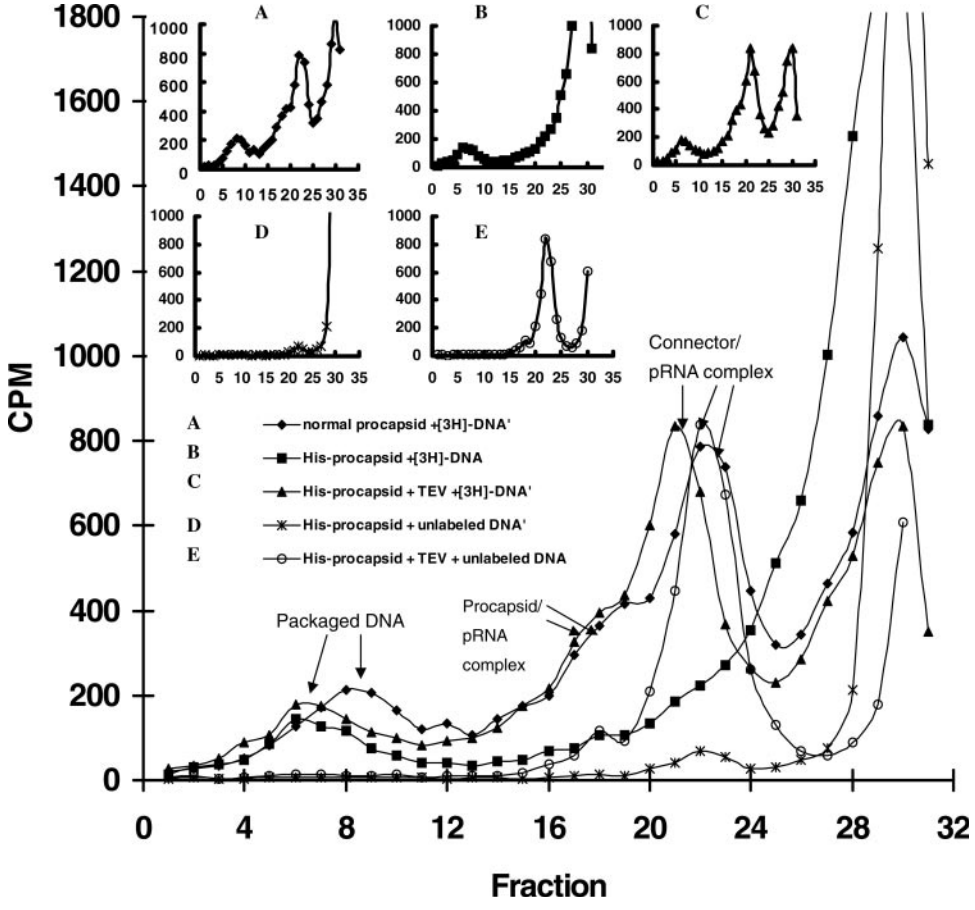

Figure 5. Sucrose gradient sedimentation (5–20%) to detect the binding of His-procapsid with [^{3}H]pRNA and the subsequent DNA-packaging using [^{3}H]pRNA *Sph* I I-i′ and [^{3}H]phi29 DNA at the same time.

was also switched on by the removal of the 20 amino acids via proteolytic cleavage with TEV. After TEV cleavage the DNA-packaging efficiency of the His-procapsid was found to be similar to the activity of wild-type procapsid when using pRNA I-i′, *Sph* I I-i′, pRNA A-a′, *Sph* I A-a′, *Sph* I E-e′ or *Sph* I A-b′+ *Sph* I B-a′ in the packaging assay (Figure 5 and 6B). It was also found that the virion assembly activity was restored after the removal of the 20 amino acids by

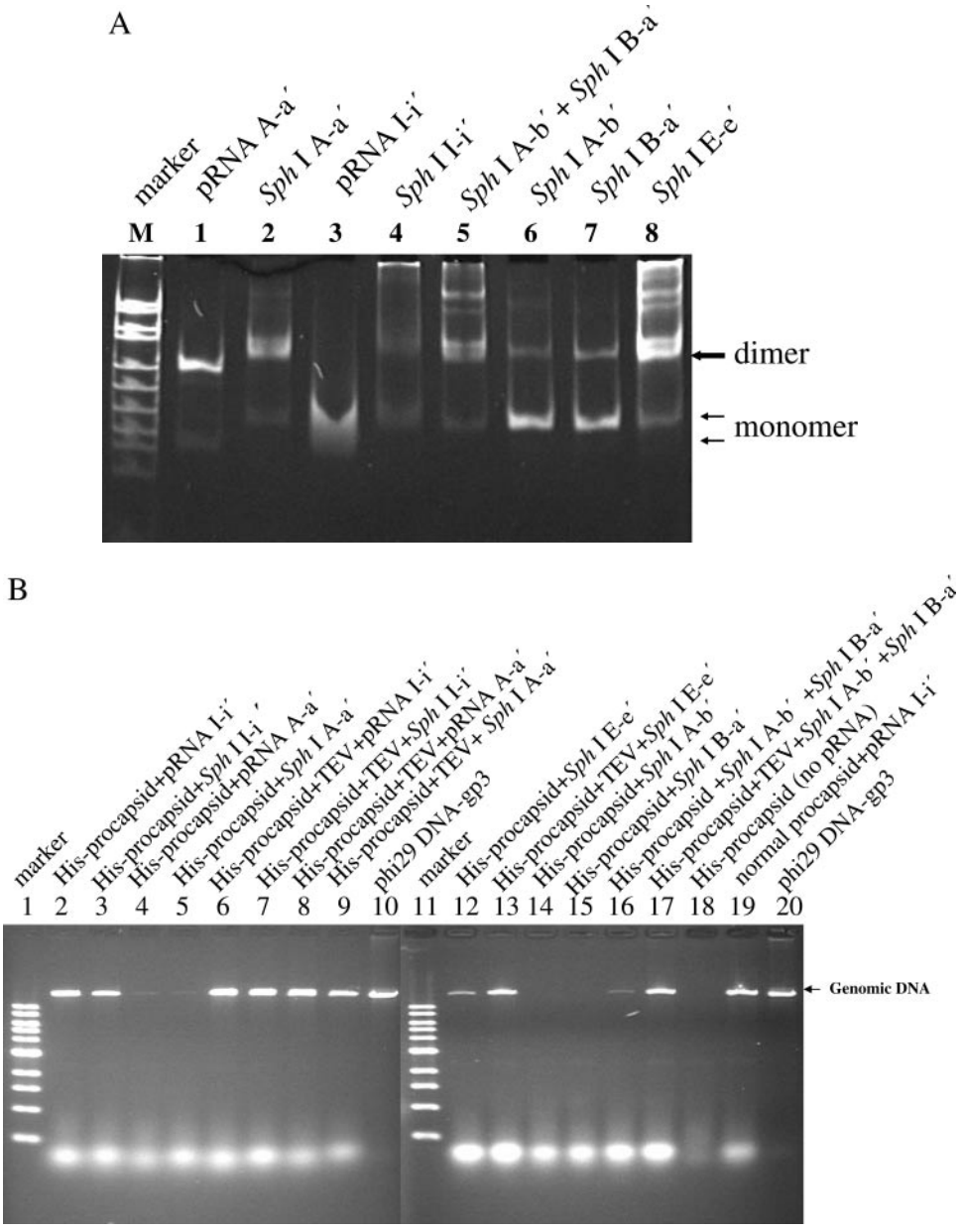

Figure 6. Comparison of DNA-packaging activity with pRNA dimer and monomer using His-procapsid. (**A**) Native gel assay (8%) for the efficiency in dimer formation and (**B**) agarose gel assay for DNA-packaging efficiency.

proteolytic cleavage. The activiy of His-procapsid increased ~10-fold after TEV cleavage.

The pRNA dimers suffered more seriously by gp10 N-terminal extension than pRNA monomers in DNA-packaging

Five different species of pRNA were used in the packaging experiments (Figure 1D). The DNA-packaging activity of pRNA A-a′, E-e′ and (A-b′) (B-a′) which exists almost as pure dimer in solution (Figures 1C and 6A, lanes 1, 2, 5 and 8), displayed greater influence for His-procapsid (Figure 6B, lanes 4, 5, 12 and 16), in comparison to pRNA I-i′, or *Sph* I I-i′ (Figure 6B, lanes 2 and 3), which exist as a partial monomer (Figure 6A, lanes 3 and 4) before assembly into procapsid. Physically the pRNA dimer is longer than pRNA monomer. The longer the polymer, the more it would be affected by the barricade spatially and physically. We speculate that such decrease in packaging activity may be due to the dramatically decreased binding efficiency between pRNA and the connector. The physical hindrance by pRNA size is greater for dimers than monomers, while the binding to the connector was blocked by the extended tag. This hindrance was removed and activity was restored after TEV cleavage (Figure 6B, lanes 8, 9, 13 and 17). Coinciding with DNA-packaging efficiency, His-procapsid also showed higher assembly activity when the partially monomeric pRNA I-i′ or *Sph* I I-i′ were used in the phi29 assembly

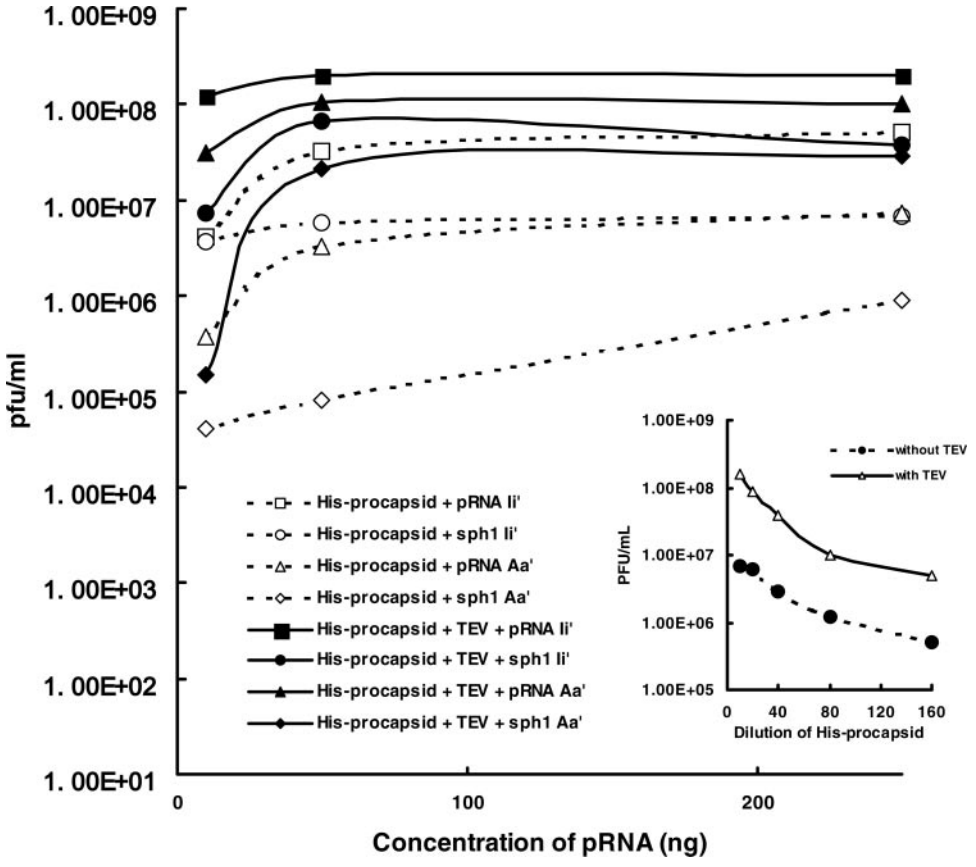

Figure 7. Comparison of the virion assembly activity of His-procapsid before and after TEV cleavage with different pRNA in *in vitro* phi29 assembly system. The inset is the assembly activity of His-procapsid with serial dilution before and after TEV cleavage using *Sph* I I-i′.

system (Figure 7). However, almost identical virion assembly activity of pRNA dimers and monomers were observed after the removal of His-tag from His-procapsid (Figure 7).

The pRNA is essential to DNA-packaging by the His-procapsid

As noted, the DNA-packaging activity of the His-procapsid was not affected by the His-tag insertion as seriously as pRNA binding. The decrease in pRNA binding to His-procapsid did not show direct correlation with inhibition of phage assembly. This would raise a question of whether the His-tagged procapsid requires the pRNA for DNA-packaging. Further testing from the RNase digestion of the purified procapsid/pRNA complex (Figure 8) reveals that virion assembly was significantly blocked after RNase digestion. This is an indication that the pRNA is still required for the DNA-packaging into the His-tagged procapsid.

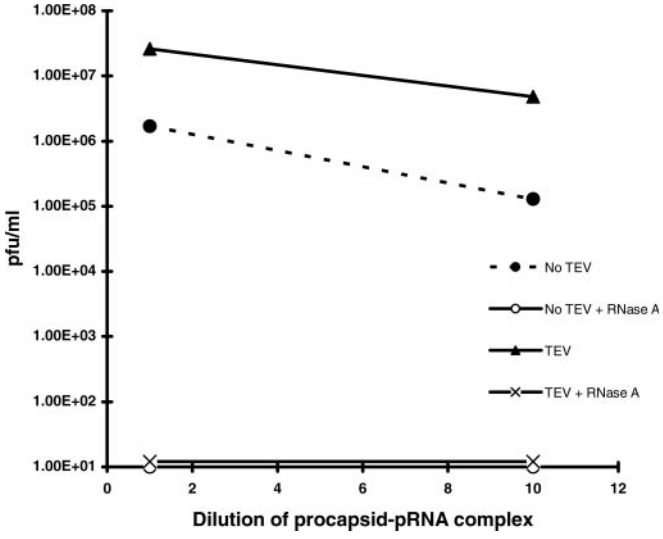

Figure 8. Assembly activity of His-procapsid–pRNA complex (after purification in 10% sucrose gradient to remove free pRNA) treated with RNase A. No assembly activity can be found after treated with RNase A.

DISCUSSION

It was found that fusion of 20 amino acids to the N-terminus of each subunit of the connector protein gp10 did not interfere with procapsid assembly and did not affect the morphology of the prolate-shape procapsid, but the binding of pRNA to the His-procapsid was dramatically decreased and the assembly of phi29 virion was inhibited. However, such decreased activity in pRNA binding and DNA-packaging were restored via proteolytic cleavage with TEV. This result implied that the amino acid residues or carried charges at the N-terminus of the connector are critical for

pRNA binding, this is in agreement with the recent finding (22), which showed that the removal of the N-terminal 14 amino acids of the gp10 protein by proteolytic cleavage resulted in undetectable binding of pRNA to either the connector or the procapsid.

It was also shown that pRNA dimers suffer more seriously from gp10 N-terminal extension than pRNA monomers in DNA-packaging. The DNA-packaging activity of pRNA dimer A-a′ (Figure 6A) showed greater influence in comparison to the partial monomer I-i′, or *Sph* I I-i′ (Figure 6A) for His-procapsid. We propose that such a decrease in DNA-packaging activity for His-procapsid compared to wild-type is due to the physical barrier effect of an extended tag from the connector, which blocked the binding of pRNA to the N-terminus of the connector and generated greater hindrance for pRNA dimers than monomers due to the size.

As noted, the insertion of a His-tag to the N-terminal of gp10 significantly interfered with the binding of pRNA to procapsid, resulting in almost undetectable binding of pRNA to procapsid by sucrose gradient sedimentation (Figure 4). However, the DNA-packaging activity of the His-procapsid was not affected by the N-terminal extensions as seriously as pRNA binding. It is possible that the binding of pRNA to the connector was less stable because of the physical hindrance of an additional His-tag from the connector. The binding was actually happening during the DNA-packaging process when the motor was turning with the supply of ATP as the energy source. However, when the motor was not in the active mode, the complex of pRNA/His-procapsid was much less stable than the pRNA/procapsid complex that it may dissociate during the sucrose gradient. The question of if the His-tagged procapsid requires the pRNA for DNA packaging was answered by further testing with RNase digestion (Figure 8), and the results showed that the pRNA is still required for DNA-packaging of the His-tagged procapsid. The other possible explanation for disproportion between pRNA binding and DNA-packaging is that the DNA-packaging activity was enhanced by the His-tag insertion as long as pRNA binding occurred, a conclusion deduced by the inhibition rate of pRNA binding and DNA-packaging using the His-tagged procapsid. This conclusion is not contradictory to the finding that phi29 assembly was inhibited by the N-terminal extension (Figure 7). The connector is the junction between procapsid and the tail. It makes sense that additional amino acids at the outer edge of the connector could affect the assembly of the tail and subsequently block the assembly of infectious virions.

The assembly of phi29 virion was inhibited by the N-terminal extension of 20 amino acids, suggesting that factors involved in virion assembly can be targets for specific antiviral treatment (28–30). For example, a chemical or peptide targeting the motor components might block viral DNA-packaging. Bacteriophage phi29 of *B.subtilis* is a linear dsDNA virus for which the DNA-packaging process has been studied in great detail. The commonality in DNA-packaging among the linear dsDNA viruses, including dsDNA bacteriophages, adenoviruses, poxviruses, and herpes viruses, implies a unique strategy of this approach for a novel drug design, wherein the attachment of a small chemical or peptide to the motor would result in specific blockage of DNA-packaging. This principle also implies a strategy for gene therapy to viral infection by expressing an extended subunit of components of the viral DNA-packaging motor. RNA viruses might use the motor to package their genomic RNA as well (31,32).

CONCLUSION

Fusion of 20 amino acids to the N-terminus of each subunit of the connector did not interfere with procapsid assembly and did not affect the morphology of the prolate-shaped procapsid, but dramatically affected the binding of pRNA to the His-procapsid and the assembly of infectious virion. However, normal motor activity was switched 'on' by the removal of the 20 amino acids via proteolytic cleavage.

ACKNOWLEDGEMENTS

The authors would like to thank Karen Rufus from Vanderbilt University for providing His-TEV expressing *E.coli* strain containing pS219V vector; Nicola Stonehouse from Leeds University for providing a plasmid pET-His-gp10; Steve Hoeprich for constructing plasmid pHis-gp7-8-8.5-10; Debra Sherman for help recording EM images; Alexander DiMauro, Songchuan Guo, Chris Williams for assistance in manuscript preparation. The research was supported by NIH grants R01-GM59944 and R01-EB03730. J.S. was supported by a fellowship from Shanghai Jiaotong University Fund. The Open Access publication charges for this article were waived by Oxford University Press.

Conflict of interest statement. None declared.

REFERENCES

1. Guo,P., Peterson,C. and Anderson,D. (1987) Prohead and DNA-gp3-dependent ATPase activity of the DNA-packaging protein gp16 of bacteriophage ϕ29. *J. Mol. Biol.*, **197**, 229–236.
2. Cue,D. and Feiss,M. (2001) Bacteriophage lambda DNA-packaging: DNA site requirements for termination and processivity. *J. Mol. Biol.*, **311**, 233–240.
3. Rao,V.B. and Black,L.W. (1988) Cloning, overexpression and purification of the terminase proteins gp16 and gp17 of bacteriophage T4: construction of a defined *in vitro* DNA-packaging system using purified terminase proteins. *J. Mol. Biol.*, **200**, 475–488.
4. Guo,P. (1994) Introduction: principles, perspectives, and potential applications in viral assembly. *Semin. Virol.*, **5**, 1–3.
5. Catalano,C.E. (2000) The terminase enzyme from bacteriophage lambda: a DNA-packaging machine. *Cell Mol. Life Sci.*, **57**, 128–148.
6. Moore,S.D. and Prevelige,P.E.,Jr (2002) DNA-packaging: a new class of molecular motors. *Curr. Biol.*, **12**, R96–R68.
7. Peterson,C., Simon,M., Hodges,J., Mertens,P., Higgins,L., Egelman,E. and Anderson,D. (2001) Composition and mass of the bacteriophage phi29 prohead and virion. *J. Struct. Biol.*, **135**, 18–25.
8. Shu,D., Huang,L. and Guo,P. (2003) A simple mathematical formula for stoichiometry quantitation of viral and nanobiological assemblage using slopes of log/log plot curves. *J. Virol. Meth.*, **115**, 19–30.
9. Meijer,W.J., Horcajadas,J.A. and Salas,M. (2001) Phi29 family of phages. *Microbiol. Mol. Biol. Rev.*, **65**, 261–287.
10. Guo,P., Erickson,S. and Anderson,D. (1987) A small viral RNA is required for *in vitro* packaging of bacteriophage ϕ29 DNA. *Science*, **236**, 690–694.
11. Zhang,C.L., Lee,C.-S. and Guo,P. (1994) The proximate 5′ and 3′ ends of the 120-base viral RNA (pRNA) are crucial for the packaging of bacteriophage ϕ29 DNA. *Virology*, **201**, 77–85.
12. Chen,C., Zhang,C. and Guo,P. (1999) Sequence requirement for hand-in-hand interaction in formation of pRNA dimers and hexamers to gear phi29 DNA translocation motor. *RNA*, **5**, 805–818.

13. Guo,P., Zhang,C., Chen,C., Trottier,M. and Garver,K. (1998) Inter-RNA interaction of phage phi29 pRNA to form a hexameric complex for viral DNA transportation. *Mol. Cell*, **2**, 149–155.
14. Trottier,M. and Guo,P. (1997) Approaches to determine stoichiometry of viral assembly components. *J. Virol.*, **71**, 487–494.
15. Zhang,F., Lemieux,S., Wu,X., St.-Arnaud,S., McMurray,C.T., Major,F. and Anderson,D. (1998) Function of hexameric RNA in packaging of bacteriophage phi29 DNA *in vitro*. *Mol. Cell*, **2**, 141–147.
16. Valpuesta,J.M., Fernandez,J.J., Carazo,J.M. and Carrascosa,J.L. (1999) The three-dimensional structure of a DNA translocating machine at 10 Å resolution. *Structure Fold. Des.*, **7**, 289–296.
17. Guasch,A., Pous,J., Ibarra,B., Gomis-Ruth,F.X., Valpuesta,J.M., Sousa,N., Carrascosa,J.L. and Coll,M. (2002) Detailed architecture of a DNA translocating machine: the high-resolution structure of the bacteriophage phi29 connector particle. *J. Mol. Biol.*, **315**, 663–676.
18. Guo,Y., Blocker,F., Xiao,F. and Guo,P. (2005) Construction and 3D computer modeling of connector arrays with tetragonal to decagonal transition induced by pRNA of phi29 DNA-packaging motor. *J. Nanosci. Nanotech.*, **5**, 856–863.
19. Hendrix,R.W. (1978) Summetry mismatch and DNA-packaging in large bacteriophages. *Proc. Natl Acad. Sci. USA*, **75**, 4779–4783.
20. Simpson,A.A., Tao,Y., Leiman,P.G., Badasso,M.O., He,Y., Jardine,P.J., Olson,N.H., Morais,M.C., Grimes,S., Anderson,D.L. *et al.* (2000) Structure of the bacteriophage phi29 DNA-packaging motor. *Nature*, **408**, 745–750.
21. Chen,C. and Guo,P. (1997) Sequential action of six virus-encoded DNA-packaging RNAs during phage phi29 genomic DNA translocation. *J. Virol.*, **71**, 3864–3871.
22. Xiao,F., Moll,D., Guo,S. and Guo,P. (2005) Binding of pRNA to the N-terminal 14 amino acids of connector protein of bacterial phage phi29. *Nucleic Acids Res.*, **33**, 2640–2649.
23. Robinson,M.A., Wood,J.P., Capaldi,S.A., Baron,A.J., Gell,C., Smith,D.A. and Stonehouse,N.J. (2006) Affinity of molecular interactions in the bacteriophage phi29 DNA-packaging motor. *Nucleic Acids Res.*, **34**, 2698–2709.
24. Guo,P., Erickson,S., Xu,W., Olson,N., Baker,T.S. and Anderson,D. (1991) Regulation of the phage ϕ29 prohead shape and size by the portal vertex. *Virology*, **183**, 366–373.
25. Zhang,C.L., Trottier,M. and Guo,P.X. (1995) Circularly permuted viral pRNA active and specific in the packaging of bacteriophage ϕ29 DNA. *Virology*, **207**, 442–451.
26. Atkinson,M.A., Barr,S. and Timbury,M.C. (1978) The fine structure of cells infected with temperature-sensitive mutants of Herpes Simples Virus Type 2. *J. Gen. Virol.*, **40**, 103–119.
27. Lee,C.S. and Guo,P. (1994) A highly sensitive system for the *in vitro* assembly of bacteriophage ϕ29 of *Bacillus subtilis*. *Virology*, **202**, 1039–1042.
28. Guo,S., Shu,D., Simon,M. and Guo,P. (2003) Gene cloning, purification and stoichiometry quantification of phi29 anti-receptor gp12 with potential use as special ligand for gene delivery. *Gene*, **315**, 145–152.
29. Trottier,M., Zhang,C.L. and Guo,P. (1996) Complete inhibition of virion assembly *in vivo* with mutant pRNA essential for phage ϕ29 DNA-packaging. *J. Virol.*, **70**, 55–61.
30. Zhang,C.L., Garver,K. and Guo,P. (1995) Inhibition of phage ϕ29 assembly by antisense oligonucleotides targeting viral pRNA essential for DNA-packaging. *Virology*, **211**, 568–576.
31. Kainov,D.E., Pirttimaa,M., Tuma,R., Butcher,S.J., Thomas,G.J., Bamford,D.H. and Makeyev,E.V. (2003) RNA packaging device of double-stranded RNA bacteriophages, possibly as simple as hexamer of P4 protein. *J. Biol. Chem.*, **278**, 48084–48091.
32. Kainov,D.E., Tuma,R. and Mancini,E.J. (2006) Hexameric molecular motors: P4 packaging ATPase unravels the mechanism. *Cell Mol. Life Sci.*, **63**, 1095–1105.